ADVANCED ENGINEERING MATERIALS

DOI: 10.1002/adem.201500419

Selective Laser Melting of Titanium Alloys and Titanium Matrix Composites for Biomedical Applications: A Review**

By *Lai-Chang Zhang** and *Hooyar Attar**

Titanium materials are ideal targets for selective laser melting (SLM), because they are expensive and difficult to machinery using traditional technologies. After briefly introducing the SLM process and processing factors involved, this paper reviews the recent progresses in SLM of titanium alloys and their composites for biomedical applications, especially developing new titanium powder for SLM. Although the current feedstock titanium powder for SLM is limited to CP-Ti, Ti–6Al–4V, and Ti–6Al–7Nb, this review extends attractive progresses in the SLM of all types of titanium, composites, and porous structures including Ti–24Nb–4Zr–8Sn and Ti–TiB/TiC composites with focus on the manufacture by SLM and resulting unique microstructure and properties (mechanical, wear/corrosion resistance properties).

1. Introduction

The combination of low density, low Young's modulus, good mechanical properties, good corrosion resistance, and high biocompatibility makes titanium alloys one of the most desirable materials for biomedical implant materials.[1–3] Titanium alloys have much lower Young's moduli (55–110 GPa) in comparison with 316LSS (210 GPa) and Co–Cr alloys (240 GPa). However, they still have moduli much higher than bone (10–30 GPa). Such a big difference in moduli between implant made of these materials and the surrounding bone causes bone resorption around the implant, leading to implant loosening and, consequently, patient may require painful revision surgery. This biomechanical incompatibility is called "stress shielding effect." As such, implant materials should possess a modulus closer to that of the bone they replace in order to reduce the stress shielding effect. This has directed to the development of new types of titanium implant materials (including design and manufacture) having a low modulus closer to that of bone, with the aim to obtain lower stiffness without major sacrifice of other key requirements.[3–10] Many low-modulus, non-toxic β-type titanium implant materials have been developed, such as Ti–29Nb–13Ta–4.6Zr (TNTZ),[3] Ti–35Nb–7Zr–5Ta (TNZT),[9] and Ti–24Nb–4Zr–8Sn (Ti2448).[10] Another solution is to employ porous structures instead of solid materials because introducing porosity could reduce both the modulus and weight of a material with respect to solid counterparts. Furthermore, the modulus of porous structure can be manipulated easily and the bone cell in-growth can be improved in comparison to solid counterparts.[11–17] Hence, porous structures can be considered for joint replacement surgery and bone grafting.[18,19]

Titanium alloys are usually produced by solidification/casting,[20–25] powder metallurgy,[26–28] space holder technology,[29] and foaming.[30] In general, these conventional

[*] *Prof. L. C. Zhang, Dr. H. Attar*
School of Engineering, Edith Cowan University, 270 Joondalup Drive, Joondalup, Perth, Western Australia 6027, Australia
E-mail: l.zhang@ecu.edu.au; lczhangimr@gmail.com; hooyar.attar@gmail.com

[**] *This research was supported under the Australian Research Council's Discovery Projects funding scheme (DP110101653). The authors are grateful to J. Eckert, M. Calin, T. B. Sercombe, Y. L. Hao, D. Klemm, K. G. Prashanth, J. Zhang, N. Dai, V. J. Challis, A. P. Roberts, J. F. Grotowski, M. Bönisch, S. Scudino, L. Löber, and A. Funk for collaboration and K. Zhuravleva, T. Gustmann, D. Lohse, and A. Voß for technical assistance. The manuscript is amended after first online publication.*

 © 2015 WILEY-VCH Verlag GmbH & Co. KGaA, Weinheim

REVIEW

Lai-Chang Zhang is an Associate Professor and the Program Leader Mechanical Engineering in the School of Engineering at Edith Cowan University. After receiving his PhD in Materials Science and Engineering at the Institute of Metal Research, Chinese Academy of Sciences in 2005, Dr Lai-Chang Zhang held several positions at The University of Western Australian, University of Wollongong, IFW Dresden and Technische Universität Darmstadt. He focuses the research on the selective laser melting, titanium alloys and composites, and processing-microstructure-properties in high-performance materials.

Hooyar Attar completed his PhD in 2015. His research interests in materials science and engineering are in the areas of additive manufacturing, metallic biomaterials and light metal alloys. In recent years, he has focused on selective laser melting of titanium materials for biomedical applications. He has collaborated actively with several research institutes and he has published over 10 articles in refereed journals.

technologies involve highly time-, material-, and energy-consuming multiple processing steps. Moreover, high reactivity of titanium with oxygen and its high melting points give rise to some challenges to these typical technologies. The complexity of extraction process, difficulty of melting, problems of fabrication and machinery make titanium alloys expensive compared to many other metallic materials. The hard machinery and high cost of materials removal arising from the conventional multi-step manufacturing processes are the two main obstacles of various potential applications of titanium alloys. Near-net shape approaches are desirable to make titanium components especially with complex shapes.

Selective laser melting (SLM), one of emerging advanced additive manufacturing technologies, is providing an ideal platform for producing titanium components. It has the capability of producing near fully dense components in a range of important engineering alloys directly from computer models. SLM offers a wide range of advantages such as net shape ability for complex shapes, high material utilization, and minimal machining, making SLM an attractive alternative to produce titanium components especially with complex shapes. On the other hand, because SLM is a complex metallurgical process, an understanding of the roles of many interrelated processing parameters is required in order to produce high-density and high-quality components by SLM. This review focuses on the selective laser melting of titanium alloys and titanium matrix composites especially of new titanium alloy powder materials. In this review, a brief introduction to SLM technology and interrelated processing parameters involved is first presented. Afterwards, the SLM of solid titanium alloys and titanium matrix composites is reviewed in order to understand how highest possible dense samples are obtained without any major defects (e.g., cracks, balling effect, and/or un-melted areas). Thirdly, the SLM of titanium porous structures potential for biomedical applications is discussed. As titanium alloys are generally categorized into alpha (α), beta (β), and $\alpha + \beta$ type groups, this paper aims to briefly review the recent progresses in the SLM of these three groups of titanium materials as well as titanium matrix composites and porous structures. The unique microstructure that is produced during SLM process and the resulting advantageous mechanical properties along with corrosion resistance property are discussed. In addition, due to the limited availability of feedstock powder in titanium alloys, some progresses in developing titanium alloys powder for SLM are also discussed.

2. Selective Laser Melting (SLM) Process and Processing Parameters Involved

Traditional subtractive manufacturing processes are basically a material removal process and controlled by removing undesirable layers of a material in order to form a product with favorite shape. Unlike subtractive manufacturing processes, emerging advanced additive manufacturing technologies such as SLM are a layer-wise process in which parts are produced layer by layer by selectively full melting and consolidating the starting powder using computer-based laser beam under a protective atmosphere. SLM process firstly starts with creating a 3D model of a product using computer aided design (CAD) software, followed by mathematically sliced thin layers. Then, these thin layers are transferred to a specific SLM device in order to realize the final product on the basis of layer by layer. Afterwards, a substrate is fixed and leveled for part fabrication on the build platform. Loose powder of thin layer is deposited on the build substrate with a thickness identical to the sliced layer thickness. The powder bed is scanned and processed based on the pre-designed CAD model using pre-defined manufacturing parameters and patterns. After fabrication of the first layer, the manufacturing process is repeated for the next layers until the build of the whole component is complete.[31] The term "selective" indicates that only partial powder is processed. The term "laser" specifies that laser is applied for processing and the term "melting" shows that selected powder is melted completely. A SLM system generally contains a controlling computer system, a processing laser, an automatic powder feeder container, and main accessorial parts (e.g., inert gas system protection, roller/scrapper, and overflow container).[31] SLM offers a wide range of advantages in comparison with the common manufacturing methods, such as near-net-shape production, lower production time, high material utilization and almost no geometric constrictions, leading to fabricate complex-shape parts nearly without need

 © 2015 WILEY-VCH Verlag GmbH & Co. KGaA, Weinheim

ADVANCED ENGINEERING MATERIALS

for further post-processing.[32–35] SLM technology has attracted a great deal of attention for fabricating several types of metallic parts, which mainly include titanium,[34–36] aluminum,[32,33,37–40] steels,[41,42] superalloy,[43,44] and recently bronze materials.[45]

2.1. Processing Parameters Involved

The most primary objective in SLM process is to obtain parts with full density and free of defects. Achieving this goal is not easy because there is no mechanical pressure during SLM, which is characterized mostly by gravity and capillary forces as well as thermal effect. A large number of processing parameters are involved during SLM; therefore, appropriate control of the relating parameters leads to a product with high quality. Some parameters (such as laser wave length and laser working mode) are not varied and are determined by the SLM device itself. Also, some properties (such as viscosity and heat conductivity) of powder used are fixed, which define the boundary conditions of SLM process. In contrast, other parameters, known as manufacturing or processing parameters, should be calculated and optimized with care.[35,46–48] In general, for a given material, the laser energy density, E, applied to a certain volume of powder material during SLM is defined by:[34]

$$E = P/(v \cdot t \cdot s) \quad (1)$$

where P is the laser power (W), v is the scan speed (mm s^{-1}), t is the layer thickness (mm), and s is scan spacing (mm). The laser energy density is a function of these key factors for the densification and the quality of SLM-fabricated parts, thereby determining their properties. As seen from Equation 1, increasing laser power and/or decreasing scan speed or layer thickness or scan spacing would increase the laser energy density and therefore the temperature of the powder. A higher incident laser energy density results in a larger amount of melting and therefore higher final density. As the formation of a fully molten is essential for manufacturing fully-dense parts, sufficient laser energy density applied to powder materials is required for obtaining high density parts. In general, a minimum critical laser energy density is required to produce parts with maximum density.[34,35,46–49] For example, the critical laser energy density for SLM of fully dense commercially pure titanium (CP–Ti), Ti–6Al–4V and Ti–24Nb–4Zr–8Sn are around 120,[47,48] 120,[49] and 40 J mm^{-3},[46] respectively.

The schematic of these SLM processing parameters is shown in Figure 1.[50] During SLM, laser beam moves across the powder bed with a constant speed known as scan speed (v), which controls the time of production in SLM. In other words, higher scan speeds are required if short production time is needed. However, the maximum laser power of a specific SLM device should be considered when increasing scan speed. Layer thickness (t) defines the amount of energy and production time required to melt/consolidate a layer of powder. Layer thickness is very important as good connectivity between layers can only be possible when previously processed layers are re-melted too. The production time is reduced if larger layer thickness is applied. However, higher energy input is also required to melt thick layers completely which may cause the increase in surface roughness and reduction in dimensional accuracy. Scan spacing (s) is usually chosen as parallel lines in SLM and, therefore, it is also called "hatch space." It has been reported[34,51] that scan spacing determines the overlap of adjacent solidified tracks, thereby significantly influencing the porosities and surface roughness of SLM-produced parts. The scan spacing should be chosen carefully to ensure a good bonding of adjacent tracks. Thus, this should vary between the half width and the full width of melt pool.

Length and pattern of laser scanning vectors are other important parameters (also called "scanning strategy") in SLM process. The length of scanning vector is defined by geometry of scanning. This scanning, known as

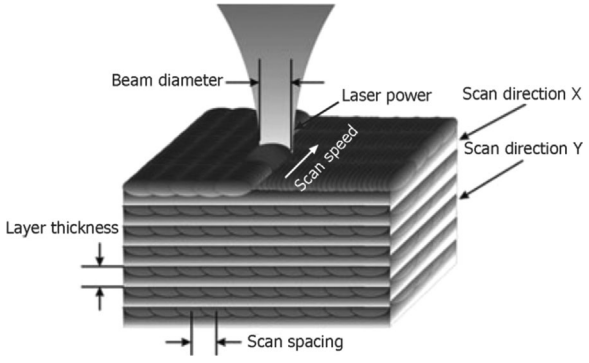

Fig. 1. Schematic of selective laser melting (SLM) parameters (modified from[50]). Reproduced with permission from Wiley [ref. no. 3690340540650].

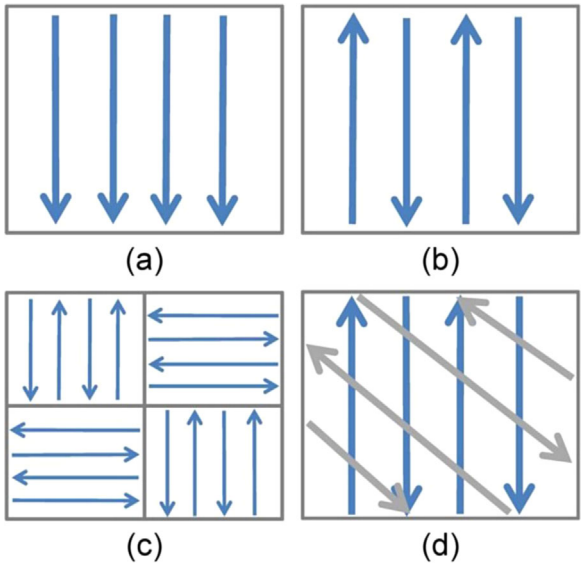

Fig. 2. Different SLM processing patterns: (a) Uni-directional scanning, (b) Bi-directional scanning (zigzag) scanning, (c) Inter-layer scanning, and (d) Interlayer rotation scanning.[34] Reproduced with permission from Elsevier [ref. no. 3690341342886].

 © 2015 WILEY-VCH Verlag GmbH & Co. KGaA, Weinheim

REVIEW

"manufacturing pattern," can be designed in different ways. The laser scan pattern typically consists of parallel and straight lines with possibility of circular or spiral coverage. The direction of scanning patterns can be changed inside a single layer or between consecutive layers. As shown in Figure 2,[34] the first two variations (Figure. 2a–b) are called uni- and bi-directional (zigzag) scanning patterns, respectively. Also, scanning direction can be rotated from section to section similar to the island scanning (inter-layer) as shown in Figure 2c. The direction of scanning can be also rotated between consecutive layers by different rotation angles (Figure 2d). The design of manufacturing pattern influences the quality of SLM-processed part.

2.2. Needs of Developing New Alloy Powder Materials for SLM

The SLM process has to deal with some parameters related to powder, laser, and scan which play important roles on the density, surface quality, microstructure and the resulting properties of the SLM-produced samples. During SLM, heat energy causes the melting/consolidation of metallic powder in which temperature can go up until evaporation temperature. Therefore, the properties of a starting material as well as specific powder characteristics are of important for the formation of melt pool and laser absorption. For example, characteristics (e.g., type, shape, size) and properties of the powder significantly affect the SLM process, powder flowability and the interaction between laser and powder material. SLM involves powder as the starting material to produce parts; therefore, the morphology of the starting powder can play a key role in determining the density and quality of the final SLM-processed products. Powder morphology defines the extent to which the particles are packed together when a new layer of powder is deposited on the previously formed solid layer. Thus, powder morphology is a crucial factor in defining the layer thickness and surface roughness during SLM process. Powder morphology relates to the shape and size of powder particles and strongly depends on the powder production methods. Ideally, powder materials with spherical shape are desirable for SLM. Spherical shaped powder materials are generally prepared by atomization. However, the chemical compositions of feedstock powder for SLM are unfortunately very limited. Currently only 29 common metal powder materials are available for SLM and among them only CP–Ti, Ti–6Al–4V and Ti–6Al–7Nb are available for titanium alloys.[52] As a result, there is a need to produce lower cost, less spherical powder materials for SLM. Ball milling (or mechanical alloying) could be an alternative technology for producing near-spherical powder materials for SLM, as it is one of low cost and powerful approaches to alloy powder mixture.[53–59] Ball-milled powder materials have been successfully used for consequent powder consolidation into bulky samples.[2,60–62] However, it is reported that long-time ball milling creates irregular-shape powder particles, which cause less compaction, thereby leading to increased porosity

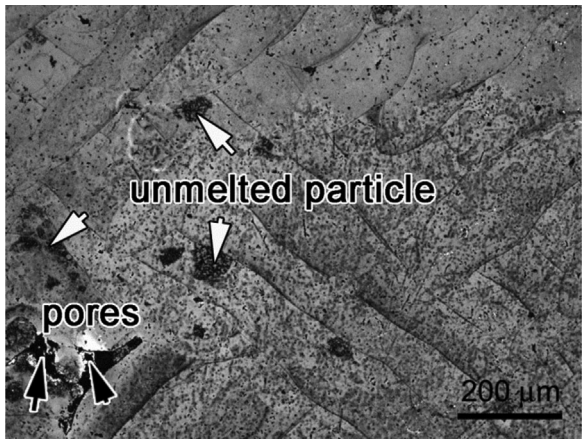

Fig. 3. Optical microstructures of the SLM-produced Ti–24Nb–4Zr-8Sn part, showing porosity and un-melted areas due to improper SLM processing parameters.[35] Reproduced with permission from Elsevier [ref. no. 3690350085655].

in the laser-fabricated parts.[63] It has been reported that optimal short milling time could produce near-spherical shape powder in titanium matrix composites[12,13,47,49,64] and oxide dispersion strengthened steel[65] for SLM process.

2.3. Unfavorable Issues and Defects in SLM

As SLM is a complex metallurgical process, the optimization of all aforementioned interrelated processing parameters is needed for producing high-density and high-quality components by SLM. As laser energy density plays a leading role in the densification of SLM-fabricated parts, defects such as unmelted areas and porosity might be created during SLM due to improper powder bed density and reduction in solubility of some elements in melt during solidification.[35,66] Figure 3 shows typical porosity and unmelted areas created during SLM processing in a β-type Ti-24Nb–4Zr–8Sn sample due to improper processing parameters.[35] Such defects could be minimized or avoid by manipulating the processing parameters.

Unfavorable issues and defects might be formed in SLM-produced parts due to localized irregularities resulting

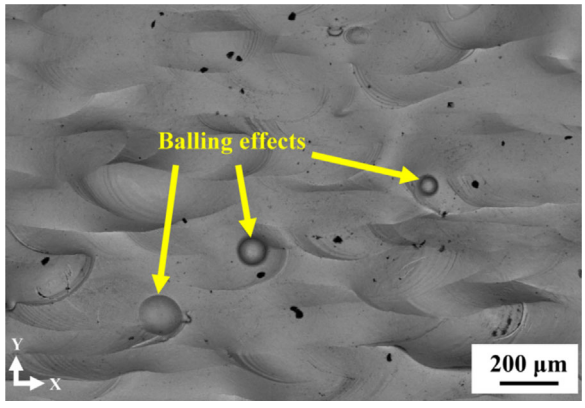

Fig. 4. Scanning electron microscopy (SEM) image showing balling effect in SLM-processed CP–Ti.[48] Reproduced with permission from Elsevier [ref. no. 3690350233765].

 © 2015 WILEY-VCH Verlag GmbH & Co. KGaA, Weinheim

from balling effect, cracks, heat affected zone (HAZ), atmospheric conditions, and residual stress. It is very important to investigate these issues in order to improve the quality and life span of SLM-processed parts. Balling effect is fragmentation or droplets resulting from melt pool due to capillary instability.[67,68] The stability of melt pool may be affected by increasing scan speed as this can cause "balling effect" in the elongated liquid pool. Balling effect, as an undesirable phenomenon related to laser-based processing, is a complex physical metallurgical process.[69] In general, during SLM, laser scanning is running line by line and laser energy causes melting in powder particles along a row, leading to the formation of a continuous liquid track with cylindrical shape. The reduction in surface energy of liquid track may continue until break-up of the cylinder in order to reach final equilibrium, causing the formation of several metallic agglomerates of spherical shape known as balling effect (Figure. 4[48]). Balling effect may cause the formation of weak interline bonding while track processing. Also, balling effect is a distinct weakness and is detrimental to uniform deposition of the next layer of the powder on the formerly processed layer, which may cause porosity as well as delamination resulting from the combination of weak interlayer bonding and thermal stresses.[69] Balling effect can be avoided if the stability of the melt pool is improved by reducing the length-to-width ratio of the melt pool and/or by increasing the contact width. To this end, for instance, higher laser power or lower scan speed can be applied. It should be noted that balling effect depends on the kinetics of the break-up process. In other words, no balling effect would take place when the time needed for break-up is longer than solidification time.

Heat affected zone (HAZ) contains the material near melt pool in which microstructure is altered due to high time and/or temperature induced. Thus, a large change in such as temperature, retention time, and/or cooling gradients occurs in heating/cooling conditions which may lead to the change in the composition and/or microstructure of HAZ, thereby influencing the quality and properties of the SLM-processed sample. Due to the additive nature of SLM process, several HAZs are caused in SLM-processed sample because of scanning of several neighboring layers. High cooling rate during SLM (10^3–$10^8\,K\,s^{-1}$[70]) leads to the formation of narrow HAZ around melt pool and large temperature gradients in HAZ. In general, HAZ should be minimized in order to reduce the inhomogeneity in the properties of SLM-produced samples. For example, large HAZ may cause the reduction in the wear resistance of SLM-produced parts.[71] The minimum HAZ could be obtained via optimal adjustment of laser processing parameters.

Cracks or any major defects are not acceptable in SLM-produced parts. In general, cracks in laser-processed samples are classified into two types, i.e., microscopic and macroscopic cracks. The microscopic cracks are usually created due to rapid solidification which is regarded normally as hot cracking. The formation of microscopic cracks is attributed to liquid film interruption at grain boundaries in the solidification temperature range due to tensile stress.[69,72] Macroscopic cracks known as cold cracking[36,73] are formed due to the low ductility of the material used itself and stress induced crack propagation. In general, microscopic and macroscopic cracks significantly reduce the dimensional accuracy and mechanical properties of SLM-produced samples. For example, defects significantly deteriorate the tensile properties of SLM-produced CP–Ti.[48]

Due to high heating/cooling rate in laser processing, residual stress is considerably high in SLM-produced components. Residual stress may result in stress cracking and interlayer de-bonding. It is reported[74] that residual stress profile usually includes large tensile stress at both top and bottom of the SLM-processed sample and intermediate compression stress at large zone in between. The magnitude and shape of residual stress are closely dependent on the material properties, height of sample, and laser processing conditions. The level of residual stress is determined by material properties especially the elastic modulus and thermal expansion coefficient (CTE). For instance, metal matrix composite material with reinforcement which has a close CTE to metal matrix is preferred. Laser processing parameters should be manipulated with care to reduce the residual stress level. Generally, residual stress is larger in the direction perpendicular to the scan direction than along scan direction.[69] Residual stress can also be controlled by preheating of the build substrate due to the decrease in temperature gradient.[75] In addition, post weld heat treatment (PWHT) can eliminate or reduce the residual stress level. Nevertheless, deep understanding is still needed to determine the effect of laser processing parameters on residual stress profile.

It is generally accepted that most metallic materials (especially titanium and its alloys) are highly reactive with surrounding atmosphere (e.g., oxygen) during SLM process. This necessitates using protective atmosphere during SLM process. In general, SLM process runs in a closed build chamber, which is commonly filled with argon under a fixed pressure in order to eliminate or reduce possibility of any contaminations especially oxidations. For example, the oxygen enrichment in the SLM-processed Ti–24Nb–4Zr–8Sn resulting from the SLM process is very small (≈0.04 wt%).[35] Nevertheless, inaccurate adjustment of gas pressure and their thermal and physical properties will influence the SLM process and cannot completely prevent oxidations. The minor surface oxidation of the particles resulting from non-optimal atmospheric conditions may pacify the surface and reduce the wettability. When oxide is stirred into the melt pool it may cause oxide entraps, leading to pores formation and weak interlayer in the SLM-produced components.[37]

3. SLM-Produced Ti-Based Materials

Titanium materials are ideal target materials for SLM because titanium materials are expensive and problematic for

 © 2015 WILEY-VCH Verlag GmbH & Co. KGaA, Weinheim

process using traditional processing technologies. From an end-user perspective, the advantages such as net shape ability for complex shapes, high material utilization, and minimal machining make SLM an attractive alternative to produce titanium components especially with complex shapes. Ti–6Al–4V has been almost the most popular and widely used titanium alloys for SLM study. Extensive endeavors have been made to study different aspects of the SLM of this alloy including the densification behavior, microstructure, and mechanical properties.[19,34,76] In addition, SLM of another ($\alpha + \beta$)-type titanium alloys such as Ti-6Al-7Nb has also been studied.[77,78] Along with Ti–6Al–4V and Ti–6Al–7Nb, β-type titanium alloys (e.g., Ti–24Nb–4Zr–8Sn and Ti–21Nb–17Zr) have been also studied.[35,79] β-type titanium alloys possess a lower Young' modulus, which reduces stress shielding effect, making them desirable for biomedical applications. In addition, the densification, microstructures and mechanical properties of CP-Ti were recently investigated.[36,48]

This Section shows that SLM technology has a great potential to fabricate different types of solid titanium materials which have comparable/superior properties to those produced using conventional techniques. Additionally, porous titanium structures with necessary features especially biomechanical properties can be fabricated by SLM. However, further investigations are still compulsory in order to develop the reliability of SLM-produced parts for biomedical applications, especially on the development of titanium alloy powder materials and the investigation of corrosion behavior and fatigue properties of SLM-produced titanium parts.

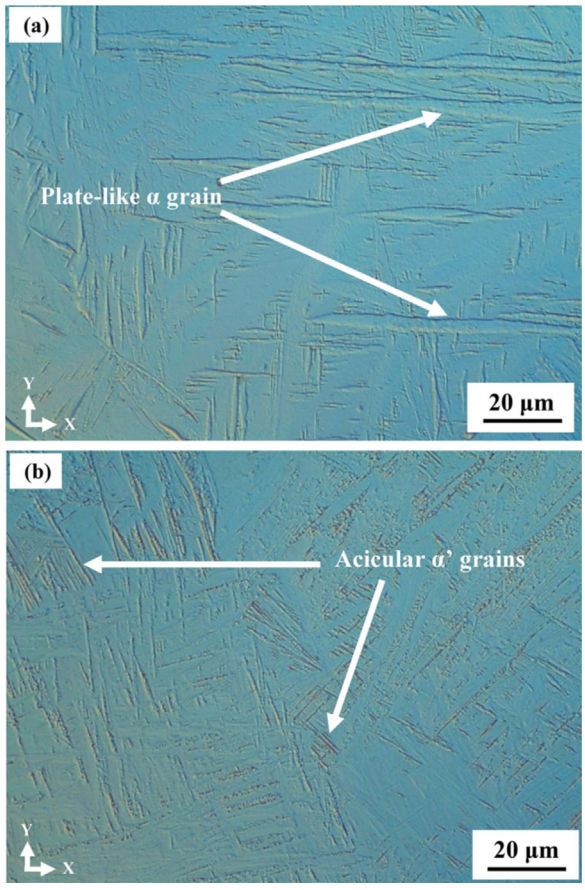

Fig. 6. Cross-sectional (Y-X) optical microstructure of the SLM-manufactured CP–Ti samples: (a) Plate-like α and (b) acicular α′.[48] Reproduced with permission from Elsevier [ref. no. 3690350233765].

3.1. SLM of α-Type CP–Ti

Commercially pure titanium (CP–Ti) is one of the most commonly used titanium materials for implant applications. SLM of CP–Ti mostly shows the importance of processing parameters on the resulting microstructure, mechanical, and wear properties.[13,18,36,48] Generally, the microstructure and mechanical properties of SLM-produced samples are closely related to the SLM processing parameters. For example, as shown in refs.,[36,48] the scan speed and laser power have significant impacts on the resulting relative density of SLM-produced samples. It is reported that the energy density (E) of 120 J mm^{-3} is sufficient to produce almost fully dense (greater than 99.5%) CP–Ti parts.[36,48] However, laser power and laser scan speed should be adjusted at this energy density for obtaining high-density parts (Figure 5[48]).

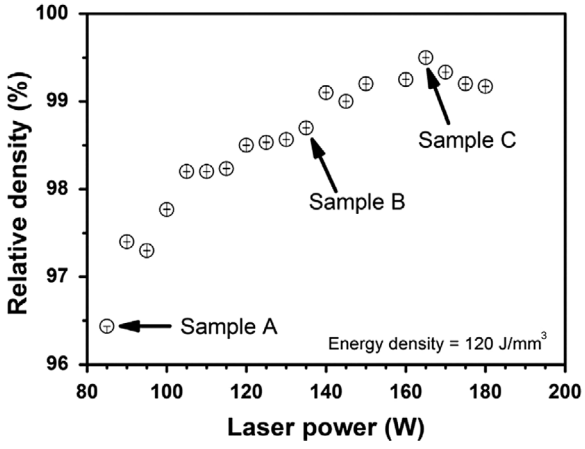

Fig. 5. Relationship between relative density and laser power for the SLM-fabricated CP–Ti parts at fixed energy density of 120 J mm^{-3}. Samples A, B, and C show different examples of relative densities.[48] Reproduced with permission from Elsevier [ref. no. 3690350233765].

Laser processing parameters influence the resulting microstructure of SLM-produced CP-Ti samples, changing from plate-like α to acicular martensitic α′ phase (Figure 6[48]) which can be attributed to different laser scan speed (v).[36] At a constant energy density (E) of 120 J mm^{-3}, when laser scan speed is less than 100 mm s^{-1} complete allotropic transformation of β to α takes place during solidification because of energy thermalization within melt pool (Figure 6a). On the other hand, on increasing the laser scan speed over 100 mm s^{-1}, both kinetic and thermal characteristics under cooling go up, causing the increase in temperature gradients within melt pool and, therefore, leading to the formation of α′ in final SLM-produced part (Figure 6b).

As shown in Table 1, the mechanical properties of SLM-produced CP–Ti including tensile and hardness

 © 2015 WILEY-VCH Verlag GmbH & Co. KGaA, Weinheim

Table 1. Comparison of Vickers hardness and tensile mechanical properties of different types of titanium alloys processed by selective laser melting and traditional methods. E is Young's modulus; $\sigma_{0.2}$ is yield strength; σ_{UTS} is the ultimate tensile strength; and ε_f is fracture strain.

Processing method	Vickers hardness [Hv]	E [GPa]	$\sigma_{0.2}$ [MPa]	σ_{UTS} [MPa]	ε_f [%]	Ref.
CP–Ti						
Selective laser melting	261 ± 13	106 ± 3	555	757	19.5	[48]
Selective laser melting	–	–	500	650	17	[18]
Sheet forming	–	–	280	345	20	[80]
Full annealed	–	–	432	561	14.7	[81]
Ti–6Al–4V						
Selective laser melting	409	109	1110	1267	7.28	[105]
Casting/superplastic forming	346	110	847	976	5.1	[1,86]
Ti–24Nb–4Zr–8Sn						
Selective laser melting	220 ± 6	53 ± 1	563 ± 38	665 ± 18	13.8 ± 4.1	[35]
Hot rolling	–	46	700	830	15.0	[89]
Hot forging	–	55	570	755	13.0	[6]

properties show that SLM can fabricate parts with superior properties to those processed by using traditional methods.[48] As evident, the yield strength ($\sigma_{0.2}$) and the ultimate tensile strength (σ_{UTS}) of SLM-produced CP–Ti are 555 and 757 MPa respectively, which are superior to the corresponding properties for sheet forming[80] and full annealed[81] conditions, and without distinct reduction in ductility. Moreover, the compressive properties of SLM-produced CP–Ti samples (1 136 MPa[48]) are higher than those of typically processed and deformed CP–Ti samples (820 and 900 MPa, respectively[82]). In addition, Vickers microhardness of SLM-processed CP–Ti samples (261 Hv[48]) is higher than that of the cast counterparts (210 Hv[83]) and is comparable with that for 55% cold rolled CP–Ti (268 Hv[84]). Such significant improvements in mechanical properties can be attributed to the grain refinement coupled with the presence of acicular α′ phase resulting from the high cooling rate occurring in SLM process.[48]

Generally, load-bearing titanium implants are usually exposed to wear. Therefore, it is essential to improve the wear properties of CP–Ti because osteolysis and aseptic loosening may occur due to poor wear resistance. As shown in ref.,[64] SLM process is also able to produce CP–Ti samples with better wear properties (in terms of lower wear rate) compared to the cast counterparts due to refined grains, martensitic microstructures, and superior microhardness.

3.2. SLM of (α + β)-Type Ti–6Al–4V and Ti–6Al–7Nb Alloys

As mentioned before, Ti–6Al–4V having an (α + β)-type microstructure is another commonly used titanium material in biomedical applications. Microstructural observations show that SLM-produced Ti–6Al–4V sample is composed of dominant fine acicular α′ martensite and some prior β grains,[34,85] unlike the typical α + β microstructure in Grade 5 sample (Figure 7[85]). Such a microstructure consisting of acicular α′ martensite rather than equilibrium α and β phases is very typical for the SLM-produced Ti–6Al–4V samples. This is ascribed to the substantially fast cooling rate during SLM (10^3–10^8 K s^{-1}[70]) than the critical cooling rate of 410 K s^{-1} required for martensitic transformation from β to α′ in Ti–6Al–4V and a substantial thermal gradient (10^4–10^5 K cm^{-1}) along the build direction in tiny melt pool resulting in columnar prior β grains. The near fully-dense SLM-produced Ti–6Al–4V parts have microhardness of 409 Hv, which is higher than that (346 Hv) of the parts processed by superplastic forming.[86] Moreover, the tensile properties of the SLM-produced and cast Ti–6Al–4V samples, as summarized in Table 1, indicate that

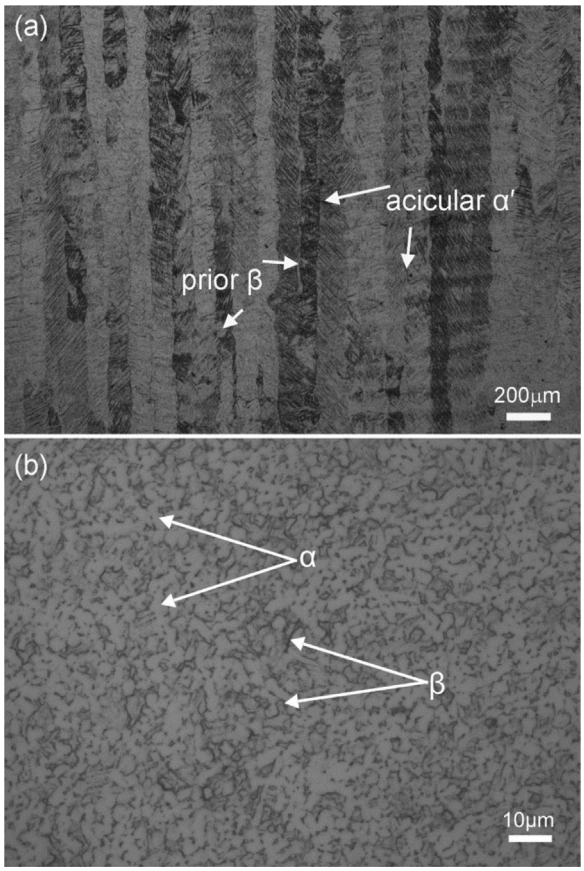

Fig. 7. Optical microstructure of the (a) SLM-produced Ti–6Al–4V sample and (b) Grade 5 alloy.[85]

 © 2015 WILEY-VCH Verlag GmbH & Co. KGaA, Weinheim

SLM-produced samples show higher yield and ultimate strengths in comparison with the cast counterparts, which can be ascribed to the martensitic microstructure formed during SLM process.[34]

The most majority studies on the SLM of metallic materials have been focused on the densification and mechanical properties of the SLM-produced samples. There is a lack of research on the corrosion behavior of SLM-produced titanium parts (and other metallic materials as well). The current research team very recently has investigated the corrosion behavior of the SLM-produced Ti–6Al–4V in 3.5 wt% NaCl solution in comparison with the commercial Grade 5 alloy.[85] Potentiodynamic measurements (Figure 8[85]) show that the corrosion current densities in the passive range of the SLM-produced Ti–6Al–4V alloy ($i_{P,B} = 0.841 \pm 0.0275\ \mu A\ cm^{-2}$) are two times those of the commercial Grade 5 alloy sample ($i_{P,A} = 0.390 \pm 0.0125\ \mu A\ cm^{-2}$). This indicates that the SLM-produced sample has unfavorable corrosion resistance than the commercial Grade 5 alloy. Furthermore, electrochemical impedance spectroscopy (EIS) experiments[85] also indicate that the fitted film resistance (R_f) of the commercial Grade 5 alloy ($94 \pm 7\ k\Omega\ cm^{-2}$) is greater than that of the SLM-produced Ti–6Al–4V sample ($40 \pm 6\ k\Omega\ cm^{-2}$). In general, a greater value of the film resistance (R_f) indicates a better corrosion resistance of the film. As such, the commercial Grade 5 alloy has better corrosion resistance than the SLM-produced Ti–6Al–4V sample. The EIS results are in good agreement with those obtained from the potentiodynamic measurements. Considering the corrosion resistance of different constituting phases, the unfavorable corrosion resistance of the SLM-produced Ti–6Al–4V sample is related to the considerably large amount of acicular α′ and less amount of β-Ti phase in the microstructure in comparison to the Grade 5 sample. The unfavorable corrosion resistance of the SLM-produced Ti–6Al–4V alloy differs from the scenario that SLM-produced samples exhibit comparable or enhanced mechanical properties compared to the counterparts prepared by traditional technologies. However, more studies on the corrosion behavior of SLM-produced titanium alloys (and other materials as well) are needed to understand the corrosion resistance of SLM-produced parts.

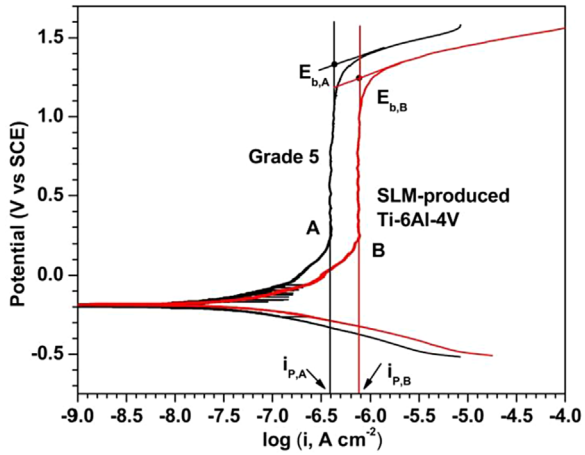

Fig. 8. Potentiodynamic curves for the SLM-produced Ti–6Al–4V alloy and commercial Grade 5 alloy in 3.5 wt% NaCl solution.[85]

SLM studies relating to (α + β)-type titanium alloys have been also performed on Ti–6Al–7Nb, which is a reformative titanium alloy to replace Ti–6Al–4V for biomedical applications. Ti–6Al–7Nb have a more favorable set of higher corrosion resistance and biocompatibility[87] and mechanical properties[88] in comparison with Ti–6Al–4V. The microstructure of SLM-produced Ti–6Al–7Nb is also composed of primarily α′ martensitic plates similar to that of Ti–6Al–4V.[77] The Vickers microhardness of the SLM-fabricated Ti–6Al–7Nb samples varies between 357 and 464 Hv, depending on the manufacturing strategy, build direction, size of β grains and α′ martensite laths and the degree of martensite decomposition.[77] Moreover, different manufacturing strategies significantly influence the mechanical properties (in terms of tensile strength) of SLM-produced samples, which can be attributed to residual stress, build defects, amount of pores and arrangement of layers with respect to tension direction during SLM process. The tensile properties of SLM-fabricated samples reach 1 440 and 1 515 MPa for yield strength and ultimate tensile strength, respectively. Due to the presence of martensitic phase in microstructure, SLM-fabricated Ti–6Al–7Nb samples exhibit better properties than wrought samples and also those obtained by thermomechanical processing.[77,86]

3.3. SLM of β-Type Ti–24Nb–4Zr–8Sn Alloy

It is well known that low-modulus, non-toxic β-type titanium alloys show low moduli closer to that of human bone and are regarded as the next generation titanium implant materials. Nevertheless, there is unfortunately no feedstock β-type titanium alloys powder available for SLM. Therefore, very little SLM work has been conducted on β-type titanium alloys. As mentioned before, Ti–24Nb–4Zr–8Sn (Ti2448) is one of good examples of biomedical β-type titanium alloys, which shows an increased balance of low modulus and high strength. The current research team has conducted some SLM studies on such novel low-modulus, non-toxic β-type titanium alloys.[16,35,46] Both Vickers mircohardness and relative density of SLM-produced Ti–24Nb–4Zr–8Sn samples are closely related to the laser processing parameters (Figure 9[35]). The density generally increases with decreasing scan speed for speeds up to ≈600 mm s^{-1}, after which the relative density tends to plateau at >99%. The critical laser energy density for SLM of fully dense Ti–24N–4Z4–8Sn is about 40 J mm^{-3},[46] which is about one third the ones for CP–Ti and Ti–6Al–4V (both around 120 J mm^{-3}[47–49]). As evident, the microhardness reaches 220 Hv for near fully dense parts. Table 1 compares the tensile properties of Ti–24Nb–4Zr–8Sn samples fabricated by SLM,[35] hot rolling[89] and hot forging.[6] It is evident that the modulus and elongation of all samples are closely comparable. On the other

 © 2015 WILEY-VCH Verlag GmbH & Co. KGaA, Weinheim

ADVANCED ENGINEERING MATERIALS

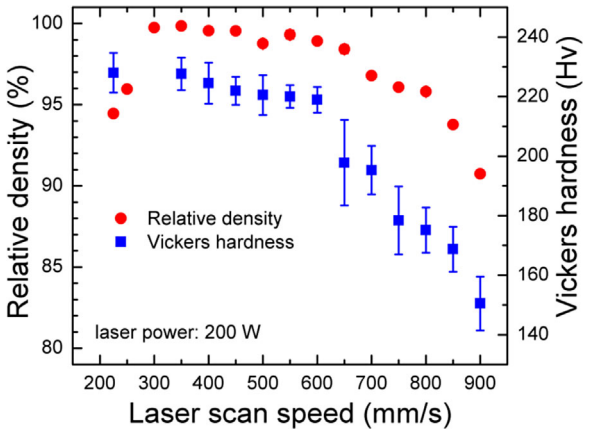

Fig. 9. Relative density and Vickers hardness of the SLM-produced Ti–24Nb–4Zr–8Sn as functions of different laser scan speeds.[35] Reproduced with permission from Elsevier [ref. no. 3690350085655].

hand, the yield and ultimate tensile strengths of SLM-produced samples are slightly lower than the corresponding ones of the parts processed by rolling and forging due to the fact that the build direction in SLM-produced samples is the weakest one compared to other directions.[35,90] Furthermore, the SLM-produced Ti–24Nb–4Zr–8Sn samples do not show the advantageous superelastic behavior as the counterparts by traditional technologies due to excessively high oxygen content in the starting powder used.[35]

3.4. SLM of Titanium Matrix Composites

In general, titanium and its alloys exhibit fairly poor hardness and wear properties. This might be unfavorable for their biomedical applications especially when the combination of high wear resistance and strength is needed (e.g., as a hip joint replacement implant). Therefore, biocompatible compounds such as TiB_2 are used in order to reinforce titanium materials as well as to improve their wear properties. Nevertheless, unfortunately no feedstock titanium matrix composites powder is available for SLM. As mentioned in Section 2.2, ball milling could be adopted for producing near-spherical titanium matrix composites powder[91] for SLM. So far, the studies on the SLM of titanium matrix composites are mainly focused on Ti–TiC and Ti–TiB composites.[12,47,49] Amongst common titanium compounds, titanium monoboride (TiB), as a reinforcement, provides advantageous properties including thermodynamic, chemical and mechanical stability. Additionally, boron is biocompatible and, hence, favorable for biomedical applications of titanium materials. Ti–TiB composites are typically formed by an in-situ reaction between titanium and titanium diboride (TiB_2), leading to the formation of Ti–TiB composite.[92,93]

Starting from the mixture of titanium powder with a spherical morphology and irregular shaped TiB_2 powder, ball milling was adopted to form Ti–TiB_2 composite powder for SLM. As spherical shaped powder is desirable for SLM, the ball-milled Ti–TiB_2 powder mixture used for SLM should be essentially homogenous and kept in an utmost spherical morphology. Figure 10 shows the resulting morphologies of the Ti–TiB_2 powder mixture after milling.[47] The Ti–TiB_2 powder ball-milled for 2 h is optimal as the starting powder for SLM because of the uniform dispersion of TiB_2 powder around the titanium matrix coupled with its almost spherical morphology (Figure 2b). Other milling times lead to either inhomogenous dispersion of TiB_2 particles around Ti powder particles (Figure 2a) or undesirably pronounced flattening of the Ti–TiB_2 powder particles (Figure 2c–d), which are not suitable for SLM.[47,94]

The typical microstructure of the SLM-produced Ti–TiB composite (Figure 11[47]) shows that TiB particles with needle-shape morphology are distributed homogeneously in α matrix. Such a microstructure is ascribed to that TiB particles display higher growth speed in $[010]_{B27}$ compared to other directions.[47] In addition, X-ray diffraction (XRD) results confirm that whole 5 wt% TiB_2 reacts with titanium during SLM to form Ti-8.35 vol% TiB composite material. Table 2 compares the Vickers microhardness and compressive properties of the SLM-produced Ti–TiB composite with those of typical titanium implant materials manufactured/processed by different technologies. As can be seen, the average microhardness value for the Ti–TiB composite is greater than those for CP–Ti and Ti–6Al–4V. The enhancement in the microhardness of Ti–TiB can be related to the hardening effect resulting from TiB particles and refinement of α-Ti grains. Moreover, the mechanical properties of the SLM-fabricated Ti–TiB composite obtained by compression testing show that the yield strength and ultimate strength of Ti–TiB are greater than the corresponding ones of CP–Ti and Ti–6Al–4V. This improvement originates from the strengthening effect of TiB

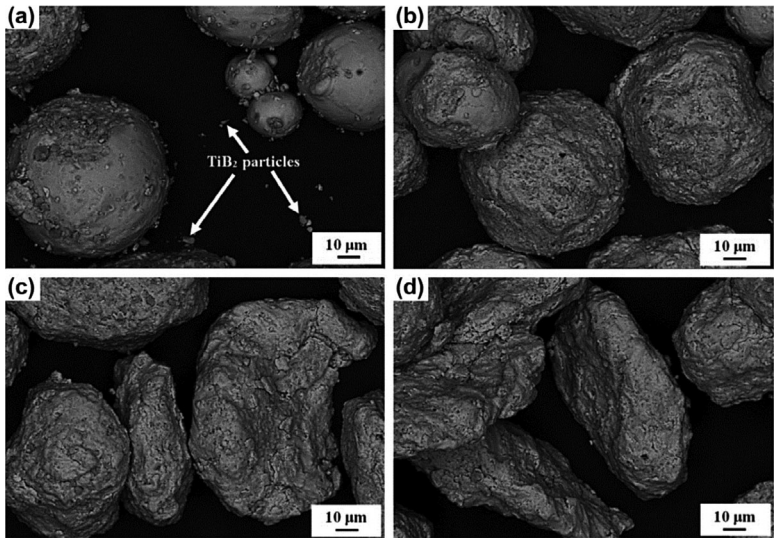

Fig. 10. Scanning electron microscopy (SEM) backscattered electron images illustrating the particle morphology of Ti–TiB_2 powder mixture ball-milled for different time: (a) 1 h, (b) 2 h, (c) 3 h, and (d) 4 h.[47] Reproduced with permission from Elsevier [ref. no. 3690350512654].

 © 2015 WILEY-VCH Verlag GmbH & Co. KGaA, Weinheim

REVIEW

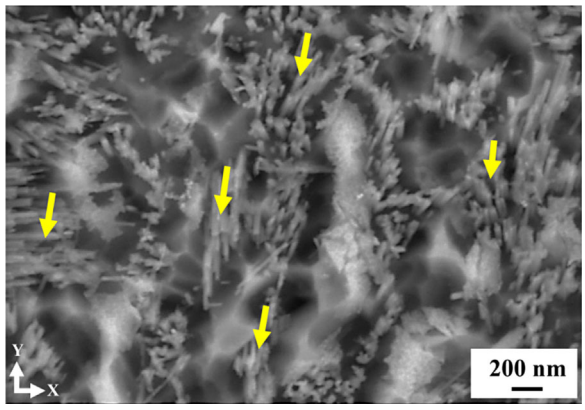

Fig. 11. Scanning electron microscopy (SEM) microstructure of the SLM-produced Ti–TiB composite. TiB particles are arrowed.[47] Reproduced with permission from Elsevier [ref. no. 3690350512654].

particles. As highlighted in ref.,[95] high yield strength improves the capacity of a material against permanent shape change which would benefit for patient. On the other hand, as reported in ref.,[12] TiB increases the Young's modulus of Ti–TiB which is not desirable for bone replacement. Regarding the SLM-produced Ti–TiC composites, due to the strengthening effect by homogeneous dispersion of nanostructured TiC reinforcement, SLM-processed TiC/Ti parts show about 22.7-fold the dynamic hardness and about 2.4-fold the elastic modulus of the unreinforced titanium part.[49]

3.5. SLM of Porous Titanium Structures

Like other AM processes, SLM process is widely used to produce bulky solid and lattice/porous structures.[12–16,36,79,96–98] Metallic cellular/porous structures have been widely applied for various industries such as load-bearing implants, heat transfer, impact protection, and damping.[99] The SLM technology is able to produce parts with complex shapes directly from different engineering materials (e.g., stainless steel, titanium alloy, and cobalt–chromium alloys) and also gives engineers the freedom to use the cellular materials with tailored functionality of a product with minor sacrifice of its mechanical properties.

SLM of titanium alloys has been also focused on the manufacture by SLM and the mechanical properties of porous structures. There are two main reasons for this aim. First, introducing porosity would further decrease the modulus of titanium to close to that of human bone thereby minimizing stress shielding effect. Also, porous structures enhance the in-growth between implant made of titanium materials and adjacent bone and therefore long term fixation of implant.[17,30]

The studies on the SLM of porous titanium structures are mainly related to CP–Ti, Ti–6Al–4V, Ti–Nb–Zr, and Ti–24Nb–4Zr–8Sn and their composites for fulfilling different requirements. For example, porous titanium structures with 55–75% porosity level analogous to human cancellous bone were fabricated by SLM and examined by compression testing.[100] The compressive strength of SLM-fabricated samples varies between 35 and 120 MPa. Furthermore, the design and manufacture of novel titanium structure for improving bone in-growth were conducted in refs.[14,15,101] It was demonstrated that SLM is able to produce optimized structures ideal for bone in-growth as well as the production of orthopedic devices. Moreover, porous CP–Ti and Ti–TiB composite materials with different porosity levels of 10, 17, and 37% were successfully produced by SLM.[13] The yield strength and elastic modulus of porous samples are in the range of 113–350 MPa and 13–68 GPa for CP–Ti and 234–767 MPa and 25–84 GPa for Ti–TiB composite materials, respectively, which are close to the corresponding ones of human bones, indicating that they can be considered as a potential candidate for biomedical implants.

SLM studies on porous Ti–6Al–4V alloy have been also focused on different objectives. For instance, Ti–6Al–4V scaffolds were produced by SLM[98] potential for bone tissue engineering and also human osteoblasts were cultured on scaffolds with great biocompatibility and resistance to compressive force. Moreover, as reported in ref.,[50] SLM is able to reproduce complex microscopic features from the original designs. An optimal structure-cage made of Ti–6Al–4V was produced by SLM. The average compressive modulus of tested samples is 2.97 GPa and in the range of trabecular (0.1–0.5 GPa) and cortical bone (15 GPa). Furthermore, theoretical and experimental measurements were conducted on octahedral Ti–6Al–4V porous structures in terms of compression test. It is reported[102] that there is an exponential association between porosity of octahedral porous structures in Ti–6Al–4V and experimental fracture load. The failure of porous structures is brittle via cleavage fracture.

3.6. Examples of SLM-Produced Titanium Implants

SLM can play an important role in the medical and biomedical engineering. Medical industry applies the

Table 2. Comparison of the Vickers hardness and compressive mechanical properties of SLM-produced Ti–TiB composite with typical metallic biomaterials (CP–Ti and Ti–6Al–4V). $\sigma_{0.2}$ is yield strength; σ_{UCS} is ultimate compressive strength; and ε_{max} is maximum strain.

Material type	Condition	Vickers hardness [Hv]	$\sigma_{0.2}$ [MPa]	σ_{UCS} [MPa]	ε_{max} [%]	Ref.
Ti-8.35 vol% TiB	Selective laser melting	402	1 103	1 421	17.8	[47]
CP–Ti	Casting/ECAP	210	700	900	35	[82,83]
Ti–6Al–4V	Superplastic forming/Annealed	346	1 000	1 300	10	[86,106]

 © 2015 WILEY-VCH Verlag GmbH & Co. KGaA, Weinheim

ADVANCED ENGINEERING MATERIALS

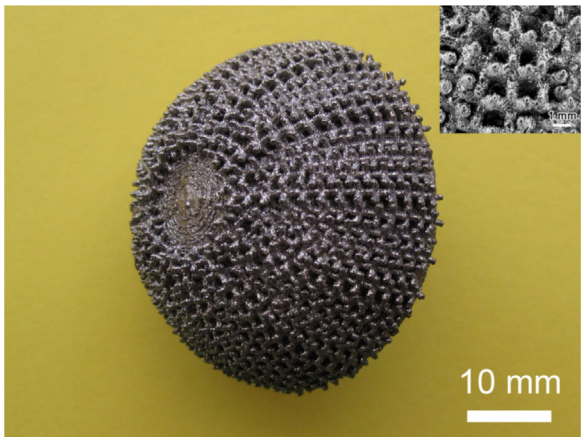

Fig. 12. An example of the SLM-produced precise Ti–24Nb–4Zr–8Sn acetabular cup.[35] Reproduced with permission from Elsevier [ref. no. 3690350085655].

advantages of SLM to manufacture different tools, implants, and devices, such as precise acetabular Ti–24Nb–4Zr–8Sn cup[35] (Figure 12). Furthermore, implants and scaffolds of titanium materials have been successfully produced by SLM for biomedical applications, which have been developed the scopes of SLM.[103,104] Studies on SLM have shown that the internal and surface finish of the implants can be tailored to be selectively porous and/or lattice-like structures to promote osseointegration (bonding between the bones and the implant) in the implants. Nowadays, several engineers/surgeries have been successful with the SLM-processed parts.

4. Conclusion

This review briefly summarizes a number of recent progresses in the most commonly used and some new titanium materials manufactured by selective laser melting (SLM) potential for biomedical applications. Firstly, a brief introduction to SLM technology, parameters involved as well as unfavorable concerns like balling effect and defects is presented. Afterwards, titanium materials and their advantages compared to the typical metallic biomaterials are described.

The relationship between SLM processing parameters and resulting microstructure and final properties of different type of titanium materials are discussed. It is also demonstrated that proper tuning of manufacturing parameters is of importance for achieving highest possible dense titanium parts and, subsequently, required mechanical properties. As reviewed, the mechanical properties of SLM-produced parts show superior features compared to those produced by common methods especially casting with only minor reduction in maximum deformation strain. However, more understanding is needed for the corrosion behavior and fatigue properties of the SLM-produced titanium parts. Moreover, the fabrication of porous titanium structures by SLM potential for biomedical purposes is also reviewed. Porous structures with mechanical and biomedical properties close to those of human bone can be successfully fabricated by SLM, indicating that SLM is not only able to produce complex-shape titanium parts but also can fulfill important requirements including longevity increase of the parts inside human bodies.

Although SLM possesses a great potential for production of titanium materials for biomedical applications, further investigations are still needed in order to ensure the reliability of the products to be used in human body and these can be possible by further understanding the processing parameters involved during SLM such as materials properties, thermal gradients, residual stress, molten liquid behavior, and surface roughness. In addition, the development of titanium alloys (also other metallic alloys) powder suitable for SLM is required urgently.

Article first published online: October 6, 2015
Manuscript Revised: September 9, 2015
Manuscript Received: August 15, 2015

[1] M. Geetha, A. K. Singh, R. Asokamani, A. K. Gogia, *Prog. Mater. Sci.* **2009**, *54*, 397.
[2] L. H. Liu, C. Yang, F. Wang, S. G. Qu, X. Q. Li, W. W. Zhang, Y. Y. Li, L. C. Zhang, *Mater. Des.* **2015**, *79*, 1.
[3] M. Niinomi, *Biomaterials* **2003**, *24*, 2673.
[4] S. E. Haghighi, H. B. Lu, G. Y. Jian, G. H. Cao, D. Habibi, L. C. Zhang, *Mater. Des.* **2015**, *76*, 47.
[5] M. Niinomi, M. Nakai, J. Hieda, *Acta Biomater.* **2012**, *8*, 3888.
[6] S. J. Li, T. C. Cui, Y. L. Hao, R. Yang, *Acta Biomater.* **2008**, *4*, 305.
[7] Y. H. Li, C. Yang, H. D. Zhao, S. G. Qu, X. Q. Li, Y. Y. Li, *Materials* **2014**, *7*, 1709.
[8] Y. Yang, G. P. Li, H. Wang, S. Q. Wu, L. C. Zhang, Y. L. Li, K. Yang, *Scripta Mater.* **2012**, *66*, 211.
[9] J. I. Qazi, B. Marquardt, L. F. Allard, H. J. Rack, *Mater. Sci. Eng. C* **2005**, *25*, 389.
[10] Y. L. Hao, S. J. Li, S. Y. Sun, C. Y. Zheng, Q. M. Hu, R. Yang, *Appl. Phys. Lett.* **2005**, *87*, 1906.
[11] X. Y. Cheng, S. J. Li, L. E. Murr, Z. B. Zhang, Y. L. Hao, R. Yang, F. Medina, R. B. Wicker, *J. Mech. Behav. Biomed. Mater.* **2012**, *16*, 153.
[12] H. Attar, M. Bönisch, M. Calin, L. C. Zhang, K. Zhuravleva, A. Funk, S. Scudino, C. Yang, J. Eckert, *J. Mater. Res.* **2014**, *29*, 1941.
[13] H. Attar, L. Löber, A. Funk, M. Calin, L. C. Zhang, K. G. Prashanth, S. Scudino, Y. S. Zhang, J. Eckert, *Mater. Sci. Eng. A* **2015**, *625*, 350.
[14] V. J. Challis, A. P. Roberts, J. F. Grotowski, L. C. Zhang, T. B. Sercombe, *Adv. Eng. Mater.* **2010**, *12*, 1106.
[15] V. J. Challis, X. X. Xu, L. C. Zhang, A. P. Roberts, J. F. Grotowski, T. B. Sercombe, *Mater. Des.* **2014**, *63*, 783.
[16] Y. J. Liu, X. P. Li, L. C. Zhang, T. B. Sercombe, *Mater. Sci. Eng. A* **2015**, *642*, 268.

 © 2015 WILEY-VCH Verlag GmbH & Co. KGaA, Weinheim

[17] G. Campoli, M. S. Borleffs, S. A. Yavari, R. Wauthle, H. Weinans, A. A. Zadpoor, *Mater. Des.* **2013**, *49*, 957.
[18] A. Barbas, A. S. Bonnet, P. Lipinski, R. Pesci, G. Dubois, *J. Mech. Behav. Biomed. Mater.* **2012**, *9*, 34.
[19] E. Sallica-Leva, A. L. Jardini, J. B. Fogagnolo, *J. Mech. Behav. Biomed. Mater.* **2013**, *26*, 98.
[20] R. Blackman, N. Barghi, C. Tran, *J. Prosth. Dent.* **1991**, *65*, 309.
[21] M. Taira, J. B. Moser, E. H. Greener, *Dent. Mater.* **1989**, *5*, 45.
[22] L. C. Zhang, J. Das, H. B. Lu, C. Duhamel, M. Calin, J. Eckert, *Scripta Mater.* **2007**, *57*, 101.
[23] M. Calin, L. C. Zhang, J. Eckert, *Scripta Mater.* **2007**, *57*, 1101.
[24] L. C. Zhang, J. Xu, *J. Non Cryst. Solids* **2004**, *347*, 166.
[25] L. C. Zhang, H. B. Lu, C. Mickel, J. Eckert, *Appl. Phys. Lett.* **2007**, *91*, 051906.
[26] G. E. Ryan, A. S. Pandit, D. P. Apatsidis, *Biomaterials* **2008**, *29*, 3625.
[27] C. Q. Ning, Y. Zhou, *Biomaterials* **2002**, *23*, 2909.
[28] A. Carman, L. C. Zhang, O. M. Ivasishin, D. G. Savvakin, M. V. Matviychuk, E. V. Pereloma, *Mater. Sci. Eng. A* **2011**, *528*, 1686.
[29] P. J. Kwok, S. M. Oppenheimer, D. C. Dunand, *Adv. Eng. Mater.* **2008**, *10*, 820.
[30] Y. J. Chen, B. Feng, Y. P. Zhu, J. Weng, J. X. Wang, X. Lu, *Mater. Lett.* **2009**, *63*, 2659.
[31] J. P. Kruth, P. Mercelis, J. Van Vaerenbergh, L. Froyen, M. Rombouts, *Rapid Prototyp. J.* **2005**, *11*, 26.
[32] K. G. Prashanth, H. S. Shahabi, H. Attar, V. C. Srivastava, N. Ellendt, V. Uhlenwinkel, J. Eckert, S. Scudino, *Add. Manuf.* **2015**, *6*, 1.
[33] K. G. Prashanth, S. Scudino, H. J. Klauss, K. B. Surreddi, L. Löber, Z. Wang, A. K. Chaubey, U. Kühn, J. Eckert, *Mater. Sci. Eng. A* **2014**, *590*, 153.
[34] L. Thijs, F. Verhaeghe, T. Craeghs, J. Van Humbeeck, J. P. Kruth, *Acta Mater.* **2010**, *58*, 3303.
[35] L. C. Zhang, D. Klemm, J. Eckert, Y. L. Hao, T. B. Sercombe, *Scripta Mater.* **2011**, *65*, 21.
[36] D. D. Gu, Y. C. Hagedorn, W. Meiners, G. Meng, R. J. S. Batista, K. Wissenbach, R. Poprawe, *Acta Mater.* **2012**, *60*, 3849.
[37] E. Louvis, P. Fox, C. J. Sutcliffe, *J. Mater. Proc. Tech.* **2011**, *211*, 275.
[38] X. J. Wang, L. C. Zhang, M. H. Fang, T. B. Sercombe, *Mater. Sci. Eng. A* **2014**, *597*, 370.
[39] X. P. Li, X. J. Wang, M. Saunders, A. Suvorova, L. C. Zhang, Y. J. Liu, M. H. Fang, Z. H. Huang, T. B. Sercombe, *Acta Mater.* **2015**, *95*, 74.
[40] X. P. Li, C. W. Kang, H. Huang, L. C. Zhang, T. B. Sercombe, *Mater. Sci. Eng. A* **2014**, *606*, 370.
[41] M. Badrossamay, T. H. C. Childs, *Int. J. Mach. Tools Manuf.* **2007**, *47*, 779.
[42] R. D. Li, Y. S. Shi, Z. G. Wang, L. Wang, J. H. Liu, W. Jiang, *Appl. Surf. Sci.* **2010**, *256*, 4350.
[43] Q. B. Jia, D. D. Gu, *J. Alloys Compd.* **2014**, *585*, 713.
[44] K. N. Amato, S. M. Gaytan, L. E. Murr, E. Martinez, P. W. Shindo, J. Hernandez, S. Collins, F. Medina, *Acta Mater.* **2012**, *60*, 2229.
[45] S. Scudino, C. Unterdörfer, K. G. Prashanth, H. Attar, N. Ellendt, V. Uhlenwinkel, J. Eckert, *Mater. Lett.* **2015**, *156*, 202.
[46] L. C. Zhang, T. B. Sercombe, *Key Eng. Mater.* **2012**, *520*, 226.
[47] H. Attar, M. Bönisch, M. Calin, L. C. Zhang, S. Scudino, J. Eckert, *Acta Mater.* **2014**, *76*, 13.
[48] H. Attar, M. Calin, L. C. Zhang, S. Scudino, J. Eckert, *Mater. Sci. Eng. A* **2014**, *593*, 170.
[49] D. D. Gu, Y. C. Hagedorn, W. Meiners, K. Wissenbach, R. Poprawe, *Compos. Sci. Tech.* **2011**, *71*, 1612.
[50] C. Y. Lin, T. Wirtz, F. LaMarca, S. J. Hollister, *J. Biomed. Mater. Res. A* **2007**, *83*, 272.
[51] I. Yadroitsev, P. Bertrand, I. Smurov, *Appl. Surf. Sci.* **2007**, *253*, 8064.
[52] J. F. Isaza, P. C. Aumund-Kopp, *Powder Metall. Rev.* **2014**, *3*, 41.
[53] P. Yu, L. C. Zhang, W. Y. Zhang, J. Das, K. B. Kim, J. Eckert, *Mater. Sci. Eng. A* **2007**, *444*, 206.
[54] L. C. Zhang, Z. Q. Shen, J. Xu, *J. Mater. Res.* **2003**, *18*, 2141.
[55] L. C. Zhang, Z. Q. Shen, J. Xu, *Mater. Sci. Eng. A* **2005**, *394*, 204.
[56] L. C. Zhang, K. B. Kim, P. Yu, W. Y. Zhang, U. Kunz, J. Eckert, *J. Alloys Compd.* **2007**, *428*, 157.
[57] C. Suryanarayana, *Prog. Mater. Sci.* **2001**, *46*, 1.
[58] H. B. Lu, C. K. Poh, L. C. Zhang, Z. P. Guo, X. B. Yu, H. K. Liu, *J. Alloys Compd.* **2009**, *481*, 152.
[59] L. C. Zhang, J. Xu, E. Ma, *J. Mater. Res.* **2002**, *17*, 1743.
[60] L. C. Zhang, J. Xu, E. Ma, *Mater. Sci. Eng. A* **2006**, *434*, 280.
[61] C. Yang, T. Wei, Y. P. Yao, Y. H. Li, S. G. Qu, L. C. Zhang, *Mater. Sci. Eng. A* **2014**, *591*, 54.
[62] L. C. Zhang, M. Calin, M. Branzei, L. Schultz, J. Eckert, *J. Mater. Res.* **2007**, *22*, 1145.
[63] J. Mazumder, D. Dutta, N. Kikuchi, A. Ghosh, *Optics Lasers Eng.* **2000**, *34*, 397.
[64] H. Attar, K. G. Prashanth, A. K. Chaubey, M. Calin, L. C. Zhang, S. Scudino, J. Eckert, *Mater. Lett.* **2015**, *142*, 38.
[65] T. Boegelein, S. N. Dryepondt, A. Pandey, K. Dawson, G. J. Tatlock, *Acta Mater.* **2015**, *87*, 201.
[66] J. P. Kruth, G. Levy, F. Klocke, T. H. C. Childs, *CIRP Ann. Manuf. Tech.* **2007**, *56*, 730.
[67] R. Morgan, C. J. Sutcliffe, W. O'Neill, *Rapid Prototyp. J.* **2001**, *7*, 159.
[68] N. K. Tolochko, S. E. Mozzharov, I. A. Yadroitsev, T. Laoui, L. Froyen, V. I. Titov, M. B. Ignatiev, *Rapid Prototyp. J.* **2004**, *10*, 78.
[69] D. D. Gu, W. Meiners, K. Wissenbach, R. Poprawe, *Int. Mater. Rev.* **2012**, *57*, 133.
[70] M. Das, V. K. Balla, D. Basu, S. Bose, A. Bandyopadhyay, *Scripta Mater.* **2010**, *63*, 438.

 © 2015 WILEY-VCH Verlag GmbH & Co. KGaA, Weinheim

ADVANCED ENGINEERING MATERIALS

[71] L. Lu, J. Y. H. Fuh, Y. S. Wong, *Laser-Induced Materials and Processes for Rapid Prototyping*, Kluwer Academic, Nowell, MA, USA **2001**.
[72] M. L. Zhong, H. Q. Sun, W. J. Liu, X. F. Zhu, J. J. He, *Scripta Mater.* **2005**, *53*, 159.
[73] J. Chen, *Appl. Laser Shanghai* **2002**, *22*, 300.
[74] P. Mercelis, J. P. Kruth, *Rapid Prototyp. J.* **2006**, *12*, 254.
[75] H. Yves-Christian, W. Jan, M. Wilhelm, W. Konrad, P. Reinhart, *Phys. Procedia* **2010**, *5*, 587.
[76] L. Facchini, E. Magalini, P. Robotti, A. Molinari, S. Höges, K. Wissenbach, *Rapid Prototyp. J.* **2010**, *16*, 450.
[77] E. Chlebus, B. Kuźnicka, T. Kurzynowski, B. Dybała, *Mater. Charact.* **2011**, *62*, 488.
[78] T. Marcu, M. Todea, I. Gligor, P. Berce, C. Popa, *Appl. Surf. Sci.* **2012**, *258*, 3276.
[79] M. Speirs, J. Van Humbeeck, J. Schrooten, J. Luyten, J. P. Kruth, *Procedia CIRP* **2013**, *5*, 79.
[80] R. Bajoraitis, *Forming of Titanium and Titanium Alloys*, Vol. *14*, ASM, **1988**.
[81] U. Bathini, T. S. Srivatsan, A. Patnaik, T. Quick, *J. Mater. Eng. Perform.* **2010**, *19*, 1172.
[82] F. W. Long, Q. W. Jiang, L. Xiao, X. W. Li, *Mater. Trans.* **2011**, *52*, 1617.
[83] C. W. Lin, C. P. Ju, J. H. C. Lin, *Mater. Trans.* **2004**, *45*, 3028.
[84] F. M. Güçlü, H. Çimenoğlu, *Mater. Sci. Forum* **2004**, *467-470*, 459.
[85] N. Dai, L. C. Zhang, J. Zhang, Q. Chen, M. Wu, *Corros. Sci.* **2015**, accepted.
[86] M. Niinomi, *Mater. Sci. Eng. A* **1998**, *243*, 231.
[87] M. F. López, A. Gutiérrez, J. A. Jiménez, *Electrochim. Acta* **2002**, *47*, 1359.
[88] X. Y. Liu, P. K. Chu, C. X. Ding, *Mater. Sci. Eng. R* **2004**, *47*, 49.
[89] S. Q. Zhang, S. J. Li, M. T. Jia, Y. L. Hao, R. Yang, *Scripta Mater.* **2009**, *60*, 733.
[90] I. Tolosa, F. Garciandía, F. Zubiri, F. Zapirain, A. Esnaola, *Int. J. Adv. Manuf. Tech.* **2010**, *51*, 639.
[91] L. C. Zhang, J. Xu, J. Eckert, *J. Appl. Phys.* **2006**, *100*, 033514.
[92] Z. Y. Ma, S. C. Tjong, L. Gen, *Scripta Mater.* **2000**, *42*, 367.
[93] K. Morsi, V. V. Patel, *J. Mater. Sci.* **2007**, *42*, 2037.
[94] H. Attar, K. G. Prashanth, L. C. Zhang, M. Calin, I. V. Okulov, S. Scudino, C. Yang, J. Eckert, *J. Mater. Sci. Tech.* **2015**, *31*, 1001.
[95] M. Calin, A. Gebert, A. C. Ghinea, P. F. Gostin, S. Abdi, C. Mickel, J. Eckert, *Mater. Sci. Eng. C* **2013**, *33*, 875.
[96] B. Vandenbroucke, J. P. Kruth, *Rapid Prototyp. J.* **2007**, *13*, 196.
[97] I. Yadroitsev, I. Shishkovsky, P. Bertrand, I. Smurov, *Appl. Surf. Sci.* **2009**, *255*, 5523.
[98] P. H. Warnke, T. Douglas, P. Wollny, E. Sherry, M. Steiner, S. Galonska, S. T. Becker, I. N. Springer, J. Wiltfang, S. Sivananthan, *Tissue Eng. C Methods* **2008**, *15*, 115.
[99] Y. Zhang, S. Ha, K. Sharp, J. K. Guest, T. P. Weihs, K. J. Hemker, *Mater. Des.* **2015**, *85*, 743.
[100] D. K. Pattanayak, A. Fukuda, T. Matsushita, M. Takemoto, S. Fujibayashi, K. Sasaki, N. Nishida, T. Nakamura, T. Kokubo, *Acta Biomater.* **2011**, *7*, 1398.
[101] L. Mullen, R. C. Stamp, W. K. Brooks, E. Jones, C. J. Sutcliffe, *J. Biomed. Mater. Res. Part B Appl. Biomater.* **2009**, *89*, 325.
[102] J. F. Sun, Y. Q. Yang, D. Wang, *Mater. Des.* **2013**, *49*, 545.
[103] N. K. Tolochko, V. V. Savich, T. Laoui, L. Froyen, G. Onofrio, E. Signorelli, V. I. Titov, *Proc. Inst. Mech. Eng. Part L J. Mat. Des. Appl.* **2002**, *216*, 267.
[104] S. Van Bael, Y. C. Chai, S. Truscello, M. Moesen, G. Kerckhofs, H. Van Oosterwyck, J. P. Kruth, J. Schrooten, *Acta Biomater.* **2012**, *8*, 2824.
[105] B. Vrancken, L. Thijs, J. P. Kruth, J. Van Humbeeck, *J. Alloys Compd.* **2012**, *541*, 177.
[106] K. Srinivasan, P. Venugopal, *Mater. Manuf. Proc.* **2008**, *23*, 342.

 © 2015 WILEY-VCH Verlag GmbH & Co. KGaA, Weinheim